PHYSICAL REVIEW B **79**, 180401(R) (2009)

Pancakelike Ising domains and charge-ordered superlattice domains in $LuFe_2O_4$

S. Park, Y. Horibe, Y. J. Choi, C. L. Zhang,* S.-W. Cheong, and Weida Wu†
Department of Physics and Astronomy and Rutgers Center for Emergent Materials, Rutgers University, Piscataway, New Jersey 08854, USA

(Received 25 January 2009; revised manuscript received 3 March 2009; published 1 May 2009)

We report magnetic and superlattice imaging of ferrimagnetic bilayered $LuFe_2O_4$ with strong uniaxial magnetic anisotropy. Magnetization reversal is imaged in magnetic fields up to 8 T at several temperatures below T_N (~230 K) and charge-ordered superlattice domains are imaged at 92 K. We observed random packing of irregular pancakelike magnetic domains (~100 nm×30 nm) and charge-ordered superlattice domains with similar shape (~30 nm×6 nm). The magnetic domain structure shows a strong memory effect in magnetization reversal. Our results are consistent with a spin-charge cross-coupling mechanism in $LuFe_2O_4$.

DOI: 10.1103/PhysRevB.79.180401 PACS number(s): 75.60.−d, 77.80.Dj, 72.80.Ga

Mixed valence compound RFe_2O_4 (R=Y, Ho, Er, Tm, Yb, and Lu) is one of the most interesting magnetic systems because of the unconventional spin and charge orderings (COs) on a geometrically frustrated lattice.[1–3] It is a magnetic system combining spin/charge frustration with low dimensionality. The RFe_2O_4 crystal consists of the alternate stacking of hexagonal Fe_2O_3 double-layer and hexagonal RO layer along the c axis, as shown in Figs. 1(a) and 1(b).[4] An equal amount of Fe^{2+} and Fe^{3+} coexists at the same site of the hexagonal (triangular) lattice. The Coulomb interaction between Fe ions prefers Fe^{2+} and Fe^{3+} as nearest neighbors, which can be effectively mapped to antiferromagnetic interaction of pseudo-Ising spins.[2] Antiferromagnetic Ising spin on triangular lattice is a geometrically frustrated system.[5] The interplay of the geometric frustration and the stacking of the triangular nets lead to a complicated hierarchy of COs.[3,6,7] $LuFe_2O_4$ has attracted a significant amount of attention because it is a possible multiferroics, where ferroelectricity and magnetism coexist.[8] Multiferroics has been the research focus of materials science because two coupled ferro-orders are of both fundamental and technological interests.[9] More interestingly, it has been suggested that the ferroelectricity in $LuFe_2O_4$ is driven by CO with broken inversion symmetry.[8–10] The cross coupling between spin and charge degrees of freedom provides an intriguing mechanism for multiferroics.[7]

In previous studies, short-range two-dimensional (2D) ferrimagnetic correlation (~5 nm) frozen below 210 K was found in $LuFe_2O_4$ by neutron scattering, indicating strong magnetic disorder.[11] Recently, Christianson *et al.*[12] observed finite three-dimensional (3D) magnetic correlations in their samples which possess long-range CO. Interestingly, they found an additional magnetic transition at 175 K and diffusive magnetic scattering along the c axis at lower temperature, which suggests emergence of magnetic disorder. A comprehensive study of bulk magnetic property, x-ray magnetic circular dichroism (XMCD), and neutron scattering from us and collaborators suggests that a freezing transition at 80 K with finite c-axis magnetic correlation is linked to the giant magnetic coercivity at low temperature.[13] This points to a possible mechanism for achieving high coercivity in magnets with strong uniaxial anisotropy.

While most of the previous studies of $LuFe_2O_4$ focused on bulk properties and reciprocal space (scattering) studies, little has been done on local properties, especially the domain structure in real space. A real-space study can provide complimentary microscopic information. In this Rapid Communication, we report magnetic and superlattice imaging of single crystals of $LuFe_2O_4$. The magnetization reversal is imaged below T_N with magnetic field up to 8 T. We observed the random configuration of pancakelike magnetic domains (~100 nm in ab plane and 30 nm along the c axis) and charge-ordered superlattice domains (~30 nm in ab plane and 6 nm along the c axis). Strong memory effect of magnetic domain pattern was found in magnetization reversal, suggesting the presence of a large amount of quenched disorder for pinning. The similar domain aspect ratios of these two types of domains suggest that the formation of the magnetic domains is strongly influenced by the preformed pancakelike CO domains (T_{CO}~310 K), probably through an

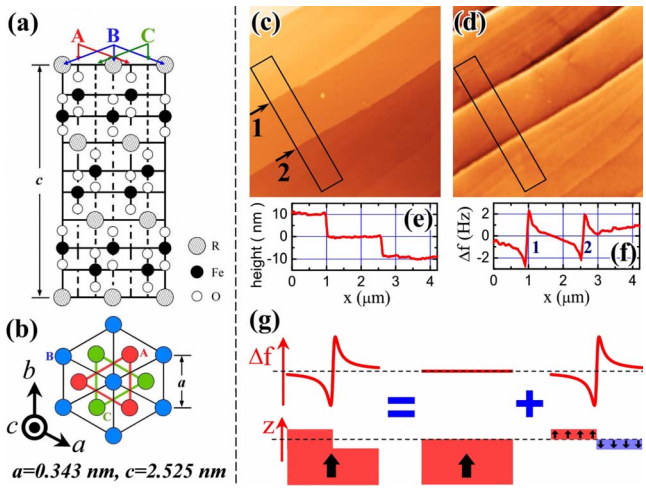

FIG. 1. (Color online) (a) Side view of the stacking of basal planes (ab planes) along the c axis of $LuFe_2O_4$. (b) Top view of the basal planes. (c) Topographic and (d) MFM images (size: ~6×6 μm^2) of one area of the cleaved surface of $LuFe_2O_4$ taken at 150 K with 8 T. The color scale is 35 nm (10 Hz) for topograph (MFM). (e) and (f) are the cross sections of the lines averaged over the boxes drawn in (c) and (d), respectively. The largest step height is about 10 nm, i.e., four times of the c-axis unit-cell size. (g) Schematic illustration. The MFM signal at a step edge of a uniform magnet is equivalent to that of a domain boundary of a thin film with uniaxial anisotropy.

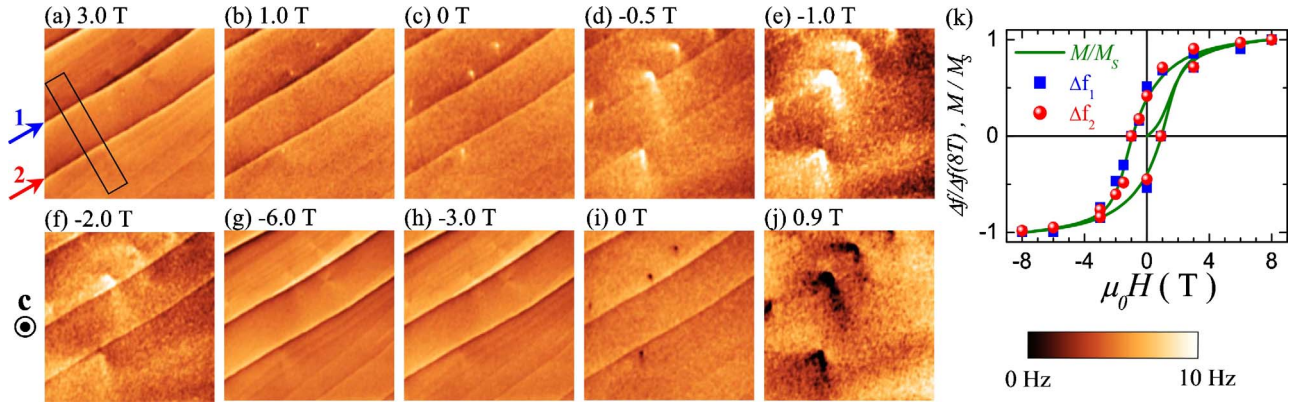

FIG. 2. (Color online) (a)–(j) MFM images taken on the same area as Fig. 1 at 150 K in magnetic fields marked in hysteresis loop in (k). The image size is $\sim 6 \times 6\ \mu m^2$. The color contrast is 10 Hz for all images. (k) Hysteresis loop of normalized magnetization M/M_s and the normalized peak-to-peak values $\Delta f/\Delta f(8\ \mathrm{T})$ of two atomic steps averaged over the rectangular box in (a).

intriguing charge-modulated spin-exchange mechanism.[7] The microscopic coexistence of spin order and charge order in $LuFe_2O_4$ is different from the mesoscopic phase separation in colossal magnetoresisitve manganites, where an intriguing cross coupling of two *competing* orders has been proposed within a phenomenological Ginzburg-Landau theory.[14]

$LuFe_2O_4$ single crystals were grown by optical floating zone method in a CO/CO_2 mixture atmosphere to control oxygen stoichiometry.[15] In this Rapid Communication, all samples are from the same sample rod, part of which was used for the previous comprehensive measurements.[13] In magnetic force microscopy (MFM) experiments, atomically flat sample surface (001) was prepared by mechanically cleaving a precut sample glued on the sample stage of a homemade variable temperature–magnetic force microscope (VT-MFM). The VT-MFM is interfaced with a Nanoscope IIIa controller (Veeco). MFM images were taken in a frequency-modulated lift mode in which the topography and MFM scan lines are interleaved. MFM tips were coated with ~ 60 nm $Co_{71}Pt_{12}Cr_{17}$ alloy by sputtering.[16] The lift heights ranged from 30 to 40 nm.[17] The sample surface was kept in cryogenic vacuum during experiment. Specimens for the transmission electron microscopy (TEM) observations were prepared by the crushing method to avoid the induction of additional oxygen defects. The TEM experiments were carried out in a JEOL-2010F operating at 200 kV and equipped with the liquid-nitrogen-cooling holder. Both the dark-field images and electron-diffraction patterns were recorded with a 14-bit charge-couple-device (CCD) array detector and imaging plates.

Figures 1(a) and 1(b) show the schematic drawings of the crystal structure of RFe_2O_4. Figures 1(c) and 1(d) show the topographic and MFM images ($\sim 6 \times 6\ \mu m^2$) on one area of the sample taken at 150 K and 8 T. The color scale of topograph (MFM) is 35 nm (10 Hz). A scale bar is displayed in Fig. 2. The sample is in saturated state at 8 T based on $M(H)$ loop in Fig. 2(k). As shown in topography, three large steps run across the field of view diagonally accompanied with a few atomic steps, suggesting a clean surface after cleaving. The sharp, dark and bright dipolar features in MFM image are aligned with step edges. They are similar to the MFM contrast from domain boundaries of uniaxial magnetic thin film. Figures 1(e) and 1(f) show the cross section of the lines averaged along the width of the boxes drawn in Figs. 1(c) and 1(d), respectively. The correlation between topography and MFM images is a result of stray field from step edges. The MFM contrast (frequency shift Δf) is approximately proportional to the magnetic interaction (force gradient $\partial_z F$) between the MFM tip and the out-of-plane component of sample stray field gradient: $\Delta f \propto \partial_z F \propto \partial_z^2 B_z$.[18] It is straightforward to show that there is no stray field gradient ($\partial_z^2 B_z = 0$) above a (infinitely large) flat surface of a uniformly magnetized magnet. A step edge of a magnet with uniform magnetization is equal to the sum of a domain boundary of a uniaxial thin film and a flat surface. Therefore, the out-of-plane stray field gradient ($\partial_z^2 B_z$) above the step edge is equivalent to that above a sharp domain boundary in a magnetic thin film, as is illustrated in Fig. 1(g). It can be shown that the peak-to-peak value of Δf is proportional to the *local* average magnetization within the magnetic interaction volume as follows:

$$\Delta f \propto \langle M \rangle_{\mathrm{local}} \tag{1}$$

for a given step height.[19] The tip-sample interaction range can be estimated by the width of the antisymmetric MFM signal, which is $\sim 1\ \mu m$.

Figure 2 shows the MFM results during magnetization reversal. Figs. 2(a)–2(j) are MFM images taken at 150 K with magnetic fields from 8 to −8 T then back to 3 T. Some images (such as 8 and 6 T) showing little change to adjacent ones are omitted for brevity. Several points can be drawn from these data. First, there are several nucleation sites within the field of view where the reversed magnetic contrast begins to emerge. It is also possible that there are similar nucleation sites beneath the sample surface, producing the weak long wavelength contrast superposition on the small dropletlike domain features. Second, the domain patterns in MFM images [Figs. 2(e) and 2(j)] taken at the coercive fields (−1.0 and +0.9 T) are almost identical except that the contrast is reversed, i.e., a strong complementary point memory effect.[20] A strong memory effect supports the presence of significant amount of quenched disorder. We note that this

domain pattern is *different* from that of conventional ferro/ferrimagnets with a strong magnetocrystalline uniaxial anisotropy, such as Co or NdFeB, where domain branching leads to flowerlike pattern.[21] Irregular domain pattern is expected in the strong disorder limit, as demonstrated in Co/Pt thin films.[20] Third, the reversed domains around nucleation sites do not have a sharp boundary with remaining area. Instead, the contrast of the reversed domains decays smoothly into the surrounding area, where weak dropletlike small features dominate. The irregular configuration of "droplets" suggests a random domain pattern. The size of dropletlike features is about 100 nm, which could be limited by our MFM lateral resolution (~50–100 nm). The weak contrast of these small domains suggests that their size along the c axis is very small. This is in agreement with neutron-scattering observation that the c-axis magnetic correlation length (~30 nm) is shorter than the in-plane one.[13]

Figure 2(k) shows the normalized hysteresis $M(H)$ loop measured by a commercial superconducting quantum interference device (SQUID) magnetometer and the normalized peak-to-peak values $[\Delta f/\Delta f(8\ \mathrm{T})]$ of the MFM signals taken at the two step edges shown in Fig. 2(a). Clearly, $\Delta f/\Delta f(8\ \mathrm{T})$ scales with bulk magnetization M, i.e., $\Delta f \propto \langle M\rangle_{\mathrm{bulk}}$. By comparing this result with Eq. (1), one could infer that

$$\langle M\rangle_{\mathrm{local}} = \langle M\rangle_{\mathrm{bulk}}. \tag{2}$$

Note that for a conventional magnet, $\langle M\rangle_{\mathrm{local}}$ equals to saturated magnetization M_s, while $\langle M\rangle_{\mathrm{bulk}}$ is usually smaller than M_s due to the presence of magnetic domains.[21] Therefore, Eq. (2) implies that the typical magnetic domain size of $LuFe_2O_4$ is much smaller than the tip-sample interaction range (~1 μm), agreeing with neutron-scattering results and previous conclusions from MFM observation.[13] This unusually small domain size implies high density of quenched disorder.[13]

So far we only discuss MFM data taken at 150 K. Similar behaviors were observed in MFM studies at 100 and 60 K, except that the saturation and coercivity fields are higher at lower temperature.[13] The domain size and pattern do not depend on temperature within our experimental uncertainty, which is consistent with the strong memory effect of magnetic domain structure and the weak and broad magnetic freezing "transition" observed in previous studies.[13] We observed similar magnetic domain pattern on three different locations. The formation of pancakelike magnetic domains (called Ising pancakes) could be caused by a weak antiferromagnetic interaction between ferrimagnetic Fe_2O_3 double layers, which would compete with ferromagnetic or dipolar interaction between these layers. Recent neutron-scattering experiments on high quality $LuFe_2O_4$ suggest a ferrimagnetic ordering with finite ferromagnetic correlation length along the c axis.[12] Unfortunately, the c-axis correlation is too complicated to rule out the antiferromagnetic correlation.[12] Alternatively, the Ising pancakes can result from a quasi-two-dimensional magnetic order interrupted by defects (quenched disorder), which also serve as pinning centers for domain boundaries between pancakes.[22] Strong memory effect also supports the presence of high density of disorder.

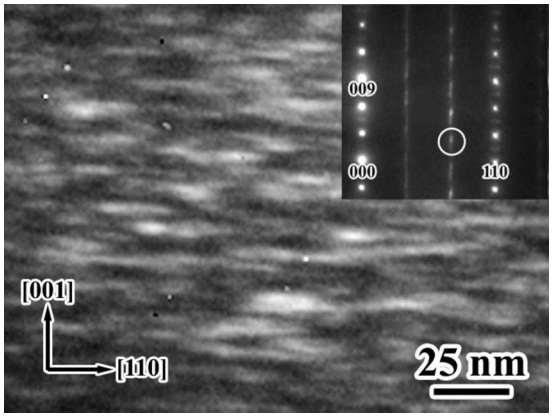

FIG. 3. High-resolution TEM dark-field image of $LuFe_2O_4$ taken at 92 K with a $(\frac{1}{3},\frac{1}{3},\frac{5}{2})$ superlattice spot, which is circled in the inset. The CO domains (bright contrast) have size of ~30 nm within the ab plane and ~6 nm along the c axis. Inset: TEM diffraction pattern of $LuFe_2O_4$ with $(1\bar{1}0)$ incidence.

The candidates of quenched disorder in $LuFe_2O_4$ include charge disorder through spin-charge coupling,[7] point defects related to ionic off-stoichiometry,[23] and structural stacking faults.[24] We found no indication of strong structural/stoichiometric defects in our samples, while synchrotron x-ray scattering determines short-range charge ordering.[13] Therefore, it is likely that charge-disordered region at the CO domain boundaries behaves as quenched disorder for the ferrimagnetic order, leading to the formation of Ising pancakes via a charge-modulated spin-exchange mechanism.[7] Previous high-resolution TEM results reveal formation of nanometer-size charge-ordered domains in YFe_2O_4 and $YbFe_2O_4$, supporting such possibility.[25,26]

Whether there is a cross coupling between charge and spin degrees of freedom is one of the key questions on multiferroic $LuFe_2O_4$. Giant magnetoelectric effects were discovered recently,[8,27] suggesting the existence of such cross coupling. Nagano *et al.*[7] proposed a charge-modulated spin-exchange scenario for spin-charge coupling, where spin frustration even enhances the CO without inversion symmetry. However, this model only consider interactions within one Fe_2O_3 bilayer, ignoring interactions between Fe_2O_3 bilayers along the c axis which seems to be important for understanding the unconventional magnetic ordering in $LuFe_2O_4$.[12,13] Nevertheless, this simple model makes an important step toward a realistic microscopic theory of spin-charge cross-coupling mechanism.

To explore the spin-charge cross-coupling phenomena in $LuFe_2O_4$, we performed high-resolution dark-field TEM imaging at low temperature on $LuFe_2O_4$ from the same sample rod used for previous studies. More than five crystallites have been studied. Figure 3 shows the typical dark-field image taken at 92 K with a $(\frac{1}{3},\frac{1}{3},\frac{5}{2})$ superlattice spot after cooling the sample with the objective lens off. Note that there is a magnetic field (~2 T) at the sample location from the objective lens during TEM observation. This field value is smaller than the coercivity at 92 K.[13] The c axis [001] is in the plane of field of view. The elliptic bright contrast is CO

superlattice domain, which suggests that they also have similar pancakelike shape as magnetic domains. The similarity indicates a strong link between the formation of pancakelike Ising domains and the CO domains. The CO domains are much smaller than the Ising domains, with size of ~30 nm in the *ab* plane and ~6 nm along the *c* axis. If there is a spin-charge coupling in $LuFe_2O_4$, charge-disordered region, e.g., CO domain boundaries naturally become quenched disorder for the ferrimagnetic correlation, disturbing and eventually interrupting the long-range magnetic correlation to finite range with similar pancake shape. In general, magnetic ordering is not sensitive to the presence of small amount of quenched disorder.[28] Empirically, CO in RFe_2O_4 is very sensitive to stoichiometry,[25] probably because of geometric frustration of Coulomb interaction in these layered materials.[1] Therefore, our results suggest that the charge-modulated spin exchange[7] offers an intriguing mechanism for the formation of nanometer-size Ising pancakes in $LuFe_2O_4$. Future studies on correlating magnetic domain pattern and CO domain pattern at the same location of samples with different CO correlation may shed more light on the spin-charge coupling mechanism in $LuFe_2O_4$.

In conclusion, we have imaged the domain structure of magnetic order and charge order and the magnetization reversal of ferrimagnetic $LuFe_2O_4$. The irregular magnetic domain size is ~100 nm in the *ab* plane and 30 nm along the *c* axis, while the CO superlattice domain size is ~30 nm in the *ab* plane and ~6 nm along the *c* axis. The random stacking of magnetic pancakes leads to an unconventional magnetic domain structure. Strong memory effect of the magnetic domain pattern suggests presence of a large amount of quenched disorder. The similar aspect ratios of magnetic and charge domains and above results are consistent with an intriguing charge-modulated spin-exchange mechanism arising from the intriguing interplay of geometric frustrations in both charge and spin sectors.[7]

We are grateful to V. Kiryukhin, P. Chandra, and K. Ahn for valuable discussions. This work was supported by Rutgers University and the NSF under Grants No. DMR-0804109 and No. DMR-0844807.

*Present address: Department of Physics, University of Tennessee Knoxville, TN 37996, USA.

†Corresponding author: wdwu@physics.rutgers.edu

[1] Y. Yamada, S. Nohdo, and N. Ikeda, J. Phys. Soc. Jpn. **66**, 3733 (1997).

[2] Y. Yamada and N. Ikeda, J. Korean Phys. Soc. **32**, S1 (1998).

[3] Y. Yamada, K. Kitsuda, S. Nohdo, and N. Ikeda, Phys. Rev. B **62**, 12167 (2000).

[4] K. Kato, I. Kawada, N. Kimizuka, and T. Katsura, Z. Kristallogr. **141**, 314 (1975).

[5] G. H. Wannier, Phys. Rev. **79**, 357 (1950).

[6] Y. Horibe, K. Kishimoto, S. Mori, and N. Ikeda, J. Korean Phys. Soc. **46**, 192 (2005).

[7] A. Nagano, M. Naka, J. Nasu, and S. Ishihara, Phys. Rev. Lett. **99**, 217202 (2007).

[8] N. Ikeda, S. Mori, and K. Kohn, Ferroelectrics **314**, 41 (2005).

[9] S.-W. Cheong and M. Mostovoy, Nature Mater. **6**, 13 (2007).

[10] J. van den Brink and D. I. Khomskii, J. Phys.: Condens. Matter **20**, 434217 (2008).

[11] J. Iida, M. Tanaka, Y. Nakagawa, S. Funahashi, N. Kimizuka, and S. Takekawa, J. Phys. Soc. Jpn. **62**, 1723 (1993).

[12] A. D. Christianson, M. D. Lumsden, M. Angst, Z. Yamani, W. Tian, R. Jin, E. A. Payzant, S. E. Nagler, B. C. Sales, and D. Mandrus, Phys. Rev. Lett. **100**, 107601 (2008).

[13] W. Wu, V. Kiryukhin, H.-J. Noh, K.-T. Ko, J.-H. Park, W. Ratcliff II, P. A. Sharma, N. Harrison, Y. J. Choi, Y. Horibe, S. Lee, S. Park, H. T. Yi, C. L. Zhang, and S.-W. Cheong, Phys. Rev. Lett. **101**, 137203 (2008).

[14] G. Milward, M. Calderón, and P. Littlewood, Nature (London) **433**, 607 (2005).

[15] J. Iida, S. Takekawa, and N. Kimizuka, J. Cryst. Growth **102**, 398 (1990).

[16] P. Grütter, D. Rugar, H. J. Main, G. Castillo, S. E. Lambert, C.-J. Lin, and R. M. Valietta, Appl. Phys. Lett. **57**, 1820 (1990).

[17] We maintained the same lift height at different temperatures by compensating for the temperature dependence of the piezoelectric coefficient of our scanner tube.

[18] D. Rugar, P. G. H. J. Main, S. E. Lambert, J. E. Stern, I. McFadyen, and T. Yogi, J. Appl. Phys. **68**, 1169 (1990).

[19] A. Wadas and P. Grütter, Phys. Rev. B **39**, 12013 (1989).

[20] M. S. Pierce, C. R. Buechler, L. B. Sorensen, J. J. Turner, S. D. Kevan, E. A. Jagla, J. M. Deutsch, T. Mai, O. Narayan, J. E. Davies, K. Liu, J. H. Dunn, K. M. Chesnel, J. B. Kortright, O. Hellwig, and E. E. Fullerton, Phys. Rev. Lett. **94**, 017202 (2005).

[21] A. Hubert and R. Schäfer, *Magnetic Domains: The Analysis of Magnetic Microstructures* (Springer Verlag, Berlin, 1998).

[22] K. Ahn (private communication).

[23] S. Funahashi, J. Akimitsu, K. Siratori, N. Kimizuka, M. Tanaka, and H. Fujishita, J. Phys. Soc. Jpn. **53**, 2688 (1984).

[24] Y. Zhang, H. X. Yang, C. Ma, H. F. Tian, and J. Q. Li, Phys. Rev. Lett. **98**, 247602 (2007).

[25] Y. Horibe, K. Kishimoto, S. Mori, and N. Ikeda, J. Electron Microsc. **54**, I87 (2005).

[26] Y. Murakami, N. Abe, T. Arima, and D. Shindo, Phys. Rev. B **76**, 024109 (2007).

[27] M. A. Subramanian, T. He, J. Chen, N. S. Rogado, T. G. Calvarese, and A. W. Sleight, Adv. Mater. **18**, 1737 (2006).

[28] J. A. Mydosh, *Spin Glasses* (Taylor & Francis, London, 1993).